

Cooperative Regions For Coded Cooperation Over Time-Varying Fading Channels

P. Castiglione¹, M. Nicoli², S. Savazzi² and Thomas Zemen¹

¹ Forschungszentrum Telekommunikation Wien, Donau-City-Strasse 1, A-1220 Vienna, Austria

² Dip. di Elettronica e Informazione, Politecnico di Milano, Piazza L. da Vinci 32, I-20133 Milano, Italy

e-mail: {castiglione, thomas.zemen}@ftw.at, {nicoli,savazzi}@elet.polimi.it

Abstract—The performance analysis of coded cooperation has been mainly focused on two extreme cases of channel variability, i.e. the block-fading (BF) and the fast-fading (FF) model. In more practical propagation environments the fading correlation across time depends on the level of user mobility. This paper analyzes the effects of time-selective fading on the performance of coded cooperation by providing an analytical framework for the error rate evaluation as a function of the mobility degree of the mobile station (MS) and of the quality of the inter-MS channel. The purpose is to evaluate the conditions on the propagation settings where the additional exploitation of spatial diversity (when time-diversity is available) provided by cooperative transmission is able to enhance substantially the performance of the non-cooperative transmission. We show that coded cooperation can outperform the non-cooperative (coded and bit-interleaved) transmission only up to a certain degree of mobility. The *cooperative region* is defined as the collection of mobility settings for which coded cooperation can be regarded as a competitive strategy compared to non-cooperative transmission. Contrary to what has been previously shown for BF channels, we demonstrate that the inter-MS channel quality plays a key role in the definition of the cooperative region.

I. INTRODUCTION

Cooperative communication [1] was originally motivated as a method to bring *spatial diversity* gain in networks of single antenna terminals through redundant transmissions from multiple mobile stations (MSs). The integration of the user cooperation idea with channel coding was then proposed in [2] to further improve the cooperative link performance. Forward error correcting (FEC) codes are used by two or more mobile stations that cooperate by transmitting to the base station (BS) incremental redundancy for the partners. This approach was shown to provide significant performance enhancements, compared to conventional non-cooperative transmission, primarily in networks with fixed or nomadic terminals: in such a situation *time diversity* cannot be exploited, while spatial diversity is beneficial as it reduces the fading impairments.

In the literature the performance analysis of coded cooperation has been mainly focused on two extreme cases of channel variability, i.e. the block-fading (BF) and the fast-fading (FF) model. However, more practical propagation environments, e.g. in vehicular networks, experience fading variations across time with a degree of correlation depending on the level of MS mobility. In these cases, temporal diversity can be exploited to improve the link reliability by the joint use of channel coding and bit-interleaved modulation [3]. Hence, it is crucial to investigate to what extent the additional exploitation of

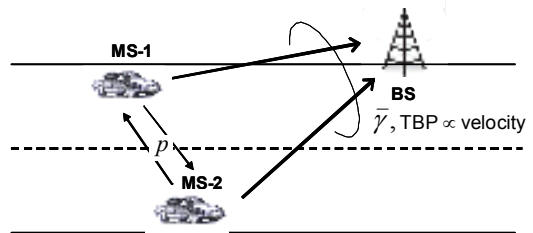


Fig. 1. System setting: the average signal-to-noise ratio (SNR) $\bar{\gamma}$ and the time-bandwidth product (TBP) of the uplink channels; the block error probability p of the inter-MS channels.

spatial diversity through collaborative transmission is able to provide substantial performance enhancements compared to non-cooperative transmission.

The contribution of this paper is twofold. Firstly, the effects of MS mobility on the performance of coded cooperation are analyzed by providing an analytical framework for the error rate evaluation as a function of the degree of fading variations. The variation degree is here measured in terms of the time-bandwidth product (TPB), that is the product of the codeword duration (for bit interleaved coded modulation) and the Doppler bandwidth. Our performance analysis is carried out in closed form and extends the results obtained by simulations in [4]. The analysis takes into account the reliability of the communication link between the cooperating MSs, by considering the block error probability p over the inter-MS link as a penalty factor that limits the cooperation performance (an overview of the system setting is shown in Fig. 1).

The above analysis is then used to evaluate the performance gain provided by coded cooperation with respect to a non-cooperative system for varying degree of MS mobility and for different channel state conditions. We show that coded cooperation can outperform the non-cooperative (coded and bit-interleaved) transmission only up to a certain degree of mobility. Beyond this limiting threshold, the temporal diversity gain, which is made available by channel coding and bit-interleaving, dominates the performances, while the spatial diversity gain offered by collaborative transmissions provides only marginal improvements. Analytical and numerical results show that the mobility degree threshold, beyond which coded cooperation is no more advantageous, decreases with the

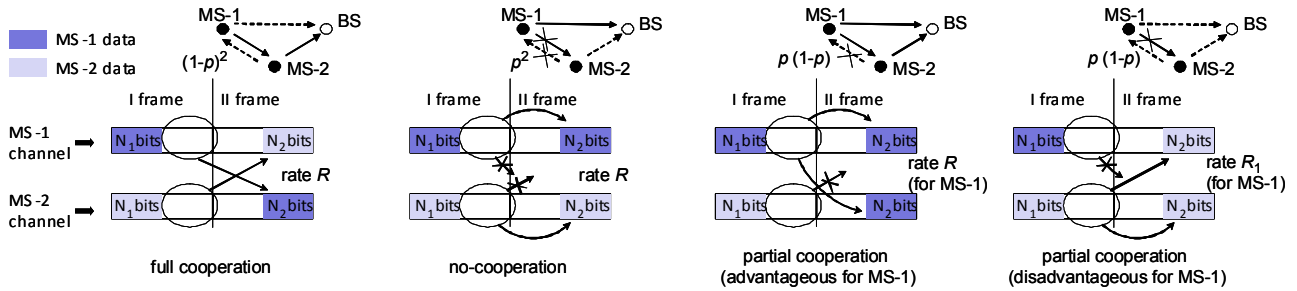


Fig. 2. Possible configurations of the coded cooperation scheme.

quality of the inter-MS channel and strongly depends on the quality of the relayed links (the uplink signal-to-noise ratio $\bar{\gamma}$ - SNR) from the cooperating MSs towards the common BS. To better highlight these results, we evaluate the *cooperative region* [5] as the collection of mobility and channel settings for which coded cooperation can be regarded as a competitive option compared to non-cooperative transmission.

The paper is organized as follows. In Section II we give a brief description of the system and the channel model. Section III presents the derivation of the analytical upperbound on the bit error rate (BER). We derive the statistical distribution of the SNR at the decision variable (here referred to as *effective SNR*) [6], based on the knowledge of the fading channel autocorrelation over the transmitted data block (a similar approach has been used for performance evaluation in frequency-selective OFDM systems [7], [8]). Section IV contains both numerical and analytical results, for the validation of the analytical BER and the investigation of the MSs' mobility effects on coded cooperation. Conclusions are drawn in Section V.

II. SYSTEM MODEL

We consider the transmission of rate- R coded data from two mobile stations, MS-1 and MS-2, towards a common BS through two orthogonal channels by frequency division multiple access (FDMA). The two channels are assumed to be subject to *independent* time-selective (due to MS mobility) frequency-flat fading. Coded cooperation is carried out according to the scheme introduced in [2], by sending portions of each MS data over the two independent channels so that a diversity gain is provided, as briefly summarized below. Each MS encodes its data block of K information bits by means of a rate-compatible punctured convolutional (RCPC) code [9] that yields an overall codeword of $N = K/R$ bits. This codeword is divided through puncturing into two sub-codewords of length N_1 and N_2 , with $N = N_1 + N_2$: the first subset is the punctured codeword of rate $R_1 = K/N_1$, the second one is the set of removed parity bits. The sub-codewords are then transmitted into two subsequent time frames. In the first frame each MS broadcasts the first sub-codeword, that is received by the cooperating partner and the BS. If the partner successfully decodes the first sub-codeword (this is determined by a cyclic redundancy check - CRC - code or any other error detection code), then it will compute and

transmit the N_2 additional parity bits in the second frame. At the BS this incremental redundancy is used for de-puncturing the rate- R_1 codeword received in the first frame, thus obtaining the initial rate- R codeword. Hence, the level of cooperation is quantified by $\alpha = \frac{N_2}{N}$. If the partner cannot successfully decode the MS' first-frame data, it will transmit its own N_2 code bits during the second frame. The latter rule avoids error propagation: each MS is forced to stop cooperating if the inter-MS transmission fails due to various possible reasons related to the inter-MS channel conditions (e.g. a deep fade, channel estimation and/or synchronization errors, etc.). Notice that even if the MSs are close and no obstacle stands on their line of sight (e.g. two vehicles running adjacently on the motorway), the media access control (MAC) protocol at one MS could anyhow decide to stop the ongoing cooperation with the partner.

Characterizing the different causes of no cooperation goes beyond the scope of the present work. Here we assume that no cooperation occurs only due to a block error event in the inter-MS transmission, with block error probability p being the same for both MSs. Furthermore, we assume, as worst case, that the inter-MS channels are independent (which is true in FDMA). Under these assumptions, four different configurations of coded cooperation can occur [2] with probability depending on the inter-MS block error rate p , as specified below (see also Fig. 2)¹:

- *Full cooperation* ($\Theta = 1$). Both MSs successfully decode each other during the first frame and can transmit the partner's code bits during the second frame. Probability: $\Pr(\Theta = 1) = (1 - p)^2$.
- *No-cooperation* ($\Theta = 2$). Both MSs fail to decode the partner's first frame and transmit their own code bits during the second frame. Probability: $\Pr(\Theta = 2) = p^2$.
- *Partial cooperation - advantageous for MS-1* ($\Theta = 3$). MS-1 cannot decode MS-2's data during the first frame, while MS-2 successfully decodes MS-1's data. During the second frame both MSs transmit the N_2 parity bits for MS-1. Probability: $\Pr(\Theta = 3) = p(1 - p)$.
- *Partial cooperation - disadvantageous for MS-1* ($\Theta = 4$). The same as the previous case, with switched MSs.

¹To simplify the reasoning, the cases of partial cooperation are described from the point of view of MS-1, while MS-2 is the partner.

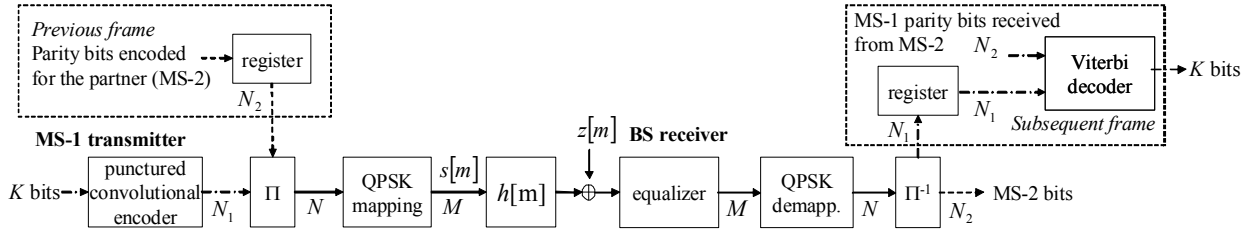


Fig. 3. Uplink system model for MS-1 successfully cooperating with MS-2.

Probability: $\Pr(\Theta = 4) = \Pr(\Theta = 3) = p(1 - p)$.

Notice that the transmission of one codeword is temporally concatenated with the transmission of the previous one (see Fig. 2). Therefore, splitting the codeword transmission into two frames does not generally modify the overall code rate R , apart from the case of partial cooperation in which the disadvantaged MS' code-rate raises to R_1 .

The complete system model is depicted in Fig. 3 for each MS-BS link (only the case $\Theta = 1$ is represented for simplicity). Bit-interleaved quadrature phase shift keying (QPSK) modulation is assumed [11] with symbol rate $1/T_S$. The baseband-equivalent discrete-time signal transmitted by MS- i , with $i \in \{1, 2\}$, is $s_i[m] = \sqrt{E_S}q_i[m]$, $m = 1, \dots, M$, where $M = N/2$ is the number of symbols per frame, E_S is the transmitted energy per symbol, and $q_i[m] = (\pm 1 \pm j)/\sqrt{2}$ is the QPSK symbol at time mT_S . The corresponding signal received at the BS is then

$$y_i[m] = h_i[m]s_i[m] + z[m], \quad (1)$$

where $z[m] \sim \mathcal{CN}(0, \sigma_n^2)$ denotes the complex additive white Gaussian noise (AWGN) at all receivers, with variance σ_n^2 . The time-variant Rayleigh-fading channel for the link between MS- i and the BS is $h_i[m] \sim \mathcal{CN}(0, \Omega_i)$ with variance Ω_i . The fading process is assumed to be wide-sense stationary (up to the second-order statistics) with Clarke's auto-correlation function given by [10]

$$R_i[k] = \mathbb{E}\{h_i[m]h_i^*[m+k]\} = \Omega_i J_0(2\pi k\nu_{D_i}), \quad (2)$$

where J_0 is the zeroth-order Bessel function of the first kind, ν_{D_i} is the one-sided normalized Doppler bandwidth $\nu_{D_i} = \frac{v_i f_C}{c_0} T_S$, v_i is the MS- i velocity, f_C the carrier frequency and c_0 the speed of light. The parameter ν_{D_i} is a measure of the temporal variability of the channel. A more meaningful parameter for coded transmissions is the time-bandwidth product, here defined as

$$\text{TBP}_i = 2M\nu_{D_i}, \quad (3)$$

where $2M$ is the temporal duration of the codeword expressed in symbol times (two frames), i.e. the time interval in which the interleaved code can exploit the temporal diversity. By definition (3), TBP represents the velocity of MS- i in terms of number of wavelengths travelled during the transmission of two frames.

According to the Rayleigh fading assumption, the instantaneous SNR, defined as

$$\gamma_i[m] = |h_i[m]|^2 \frac{E_S}{\sigma_n^2}, \quad (4)$$

exhibits an exponential distribution with mean $\bar{\gamma}_i = \Omega_i \frac{E_S}{\sigma_n^2}$ [6].

At the receiver side, coherent equalization is carried out using perfect knowledge for the channel $h_i[m]$, followed by de-mapping, de-interleaving and decoding, as illustrated in Fig. 3.

III. PERFORMANCE ANALYSIS

In the following, the derivation of the analytical upperbound on the average BER is presented. We first assume that the MSs are always cooperating, as for an error-free inter-MS channel with $p = 0$ (Sect. III-A). Then in Sect. III-B the analysis is extended to include the other cases of coded cooperation.

A. Analysis for ideal (error-free) inter-MS channel

According to the union bound approach [11], the average bit error probability, for the full cooperation case ($\Theta = 1$), P_b at the Viterbi decoder output is:

$$P_b \leq \frac{1}{k} \sum_{d \geq d_{\text{free}}} \sum_{\mathbf{c} \in \mathcal{E}(d)} \beta(\mathbf{c}) P(\mathbf{c}), \quad (5)$$

where k is the number of input bits for each branch of the convolutional code trellis, d_{free} is the free distance, $\mathcal{E}(d)$ is the set of error events \mathbf{c} at a certain Hamming distance d , $\beta(\mathbf{c})$ is the Hamming weight of the input sequence corresponding to \mathbf{c} and $P(\mathbf{c})$ is the average pairwise error probability (PEP). The average PEP $P(\mathbf{c})$ is the probability of detecting the codeword \mathbf{c} instead of the transmitted all-zero codeword.

Let $\mathcal{T}_{\mathbf{c}} = \{\tau_{\mathbf{c},1}, \dots, \tau_{\mathbf{c},d}\}$ be the set of time instants associated with the d error bits in \mathbf{c} , and $\tilde{\mathbf{h}} = \sqrt{E_S} [h(\tau_{\mathbf{c},1}) \dots h(\tau_{\mathbf{c},d})]^T / \sigma_n$ be the vector that gathers the corresponding channel gains scaled by $\sqrt{E_S}/\sigma_n$. The average PEP $P(\mathbf{c})$ can be calculated as [3]:

$$P(\mathbf{c}) = \int_0^\infty Q(\sqrt{2\gamma_{\text{eff}}}) p(\gamma_{\text{eff}}) d\gamma_{\text{eff}}, \quad (6)$$

where γ_{eff} (effective SNR) is the sum of the SNR variates that are experienced over the time instants $\mathcal{T}_{\mathbf{c}}$ [7], or, equivalently, the sum of the squared magnitudes of the vector $\tilde{\mathbf{h}}$'s entries:

$$\gamma_{\text{eff}} = \sum_{k \in \mathcal{T}_{\mathbf{c}}} \gamma(k) = \|\tilde{\mathbf{h}}\|^2. \quad (7)$$

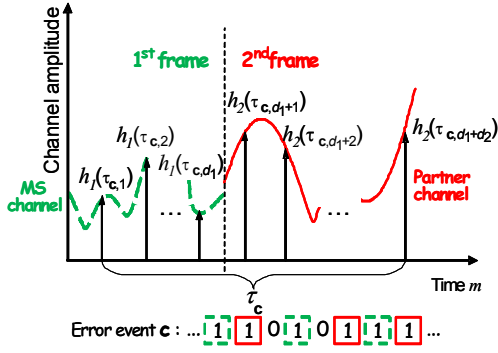


Fig. 4. Example of the correlated fading observed along the error event in the case of full cooperation ($\Theta = 1$).

Its probability density function (pdf), $p(\gamma_{\text{eff}})$, clearly depends on the correlation of the channel gains contained in $\tilde{\mathbf{h}}$. We observe that $\tilde{\mathbf{h}}$ is a zero-mean complex Gaussian random vector, $\tilde{\mathbf{h}} \sim \mathcal{CN}(\mathbf{0}, \mathbf{R}_{\mathbf{c}})$, with covariance $\mathbf{R}_{\mathbf{c}} = \mathbb{E}[\tilde{\mathbf{h}} \cdot \tilde{\mathbf{h}}^H]$ whose entries are samples of the auto-correlation function (2). The distribution of the effective SNR is here derived based on the knowledge of the correlation matrix $\mathbf{R}_{\mathbf{c}}$, by extending the approach in [8] to the cooperative scenario with time-selective fading channels.

Recalling that the codeword is partitioned into two frames due to the coded cooperation scheme, it should be observed that, for the case of full cooperation ($\Theta = 1$), the d error bits in \mathbf{c} are split into two groups of bits coming from the MS's and the partner's uplink channels (see Fig. 4). Let us consider for instance the codeword of MS-1, the time instants associated with the first and the second groups are here indicated as $\mathcal{T}_{\mathbf{c};1}$ (d_1 elements) and $\mathcal{T}_{\mathbf{c};2}$ (d_2 elements), respectively, with $\mathcal{T}_{\mathbf{c}} = \mathcal{T}_{\mathbf{c};1} \cup \mathcal{T}_{\mathbf{c};2}$. Accordingly, the channel vector is $\tilde{\mathbf{h}} = [\tilde{\mathbf{h}}_{1,d_1}^T, \tilde{\mathbf{h}}_{2,d_2}^T]^T$, where $\tilde{\mathbf{h}}_{1,d_1} = \sqrt{E_s} [h_1(\tau_{c,1}) \cdots h_1(\tau_{c,d_1})]^T / \sigma_n$ and $\tilde{\mathbf{h}}_{2,d_2} = \sqrt{E_s} [h_2(\tau_{c,d_1+1}) \cdots h_2(\tau_{c,d_1+d_2})]^T / \sigma_n$ gather the channel coefficients for, respectively, the MS-1 and MS-2 uplink channels, at time instants $\mathcal{T}_{\mathbf{c};1}$ and $\mathcal{T}_{\mathbf{c};2}$. In order to derive the effective SNR's statistical distribution, we introduce the eigenvalue decomposition (EVD) of the covariance matrices of the two channel vectors:

$$[\mathbf{R}_{\mathbf{c},1}]_{d_1 \times d_1} = \mathbb{E}[\tilde{\mathbf{h}}_{1,d_1} \cdot \tilde{\mathbf{h}}_{1,d_1}^H] = \mathbf{U}_1 \mathbf{\Lambda}_1 \mathbf{U}_1^H, \quad (8)$$

$$[\mathbf{R}_{\mathbf{c},2}]_{d_2 \times d_2} = \mathbb{E}[\tilde{\mathbf{h}}_{2,d_2} \cdot \tilde{\mathbf{h}}_{2,d_2}^H] = \mathbf{U}_2 \mathbf{\Lambda}_2 \mathbf{U}_2^H. \quad (9)$$

The matrices $\mathbf{\Lambda}_1 = \text{diag}[\lambda_{1,1}, \dots, \lambda_{1,r_1}]$ and $\mathbf{\Lambda}_2 = \text{diag}[\lambda_{2,1}, \dots, \lambda_{2,r_2}]$ contain the non-zero eigenvalues, with $r_1 = \text{rank}[\mathbf{R}_{\mathbf{c},1}]_{d_1 \times d_1} \leq d_1$ and $r_2 = \text{rank}[\mathbf{R}_{\mathbf{c},2}]_{d_2 \times d_2} \leq d_2$. \mathbf{U}_1 and \mathbf{U}_2 gather the corresponding eigenvectors. We recall that the two MS's channels are assumed to be independent, hence it is $\mathbb{E}[\tilde{\mathbf{h}}_{1,d_1} \cdot \tilde{\mathbf{h}}_{2,d_2}^H] = \mathbf{0}$ and the correlation matrix can

be written as

$$\begin{aligned} \mathbf{R}_{\mathbf{c}} &= \begin{bmatrix} [\mathbf{R}_{\mathbf{c},1}]_{d_1 \times d_1} & \mathbf{0} \\ \mathbf{0} & [\mathbf{R}_{\mathbf{c},2}]_{d_2 \times d_2} \end{bmatrix} \\ &= \underbrace{\begin{bmatrix} \mathbf{U}_1 & \mathbf{0} \\ \mathbf{0} & \mathbf{U}_2 \end{bmatrix}}_{\mathbf{U}} \underbrace{\begin{bmatrix} \mathbf{\Lambda}_1 & \mathbf{0} \\ \mathbf{0} & \mathbf{\Lambda}_2 \end{bmatrix}}_{\mathbf{\Lambda}} \underbrace{\begin{bmatrix} \mathbf{U}_1 & \mathbf{0} \\ \mathbf{0} & \mathbf{U}_2 \end{bmatrix}^H}_{\mathbf{U}^H}, \end{aligned} \quad (10)$$

where $\mathbf{\Lambda} = \text{diag}[\lambda_{1,1}, \dots, \lambda_{1,r_1}, \lambda_{2,1}, \dots, \lambda_{2,r_2}]$ collects the eigenvalues of $\mathbf{R}_{\mathbf{c}}$ and \mathbf{U} the corresponding eigenvectors. Notice that it is $r = \text{rank}[\mathbf{R}_{\mathbf{c}}] = r_1 + r_2$.

Using the EVD (10), the effective SNR can now be rewritten as $\gamma_{\text{eff}} = \|\mathbf{b}\|^2 = \sum_{i=1}^r b_i^2$, in terms of the projection of the channel onto the r -dimensional column-space of $\mathbf{R}_{\mathbf{c}}$: $\mathbf{b} = \mathbf{U}^H \tilde{\mathbf{h}} = [b_1 \cdots b_r]^T$. Notice that $\mathbf{b} \sim \mathcal{CN}(\mathbf{0}, \mathbf{\Lambda})$, thus the effective SNR is the sum of r independent exponentially distributed variates having as mean values the eigenvalues of $\mathbf{R}_{\mathbf{c}}$. It follows that the pdf of γ_{eff} exhibits the moment-generating function (MGF) [6], [12]:

$$\mathbf{M}_{\gamma_{\text{eff}}}(s) = \prod_{i=1}^{r_1} \frac{1}{1 - \lambda_{1,i}s} \prod_{j=1}^{r_2} \frac{1}{1 - \lambda_{2,j}s}. \quad (11)$$

The integral over γ_{eff} in (6) can now be derived using the alternate integral form of the Q -function [13] and the well known MGF method [12]. We get the average PEP

$$P(\mathbf{c}) = \frac{1}{\pi} \int_0^{\frac{\pi}{2}} \prod_{i=1}^{r_1} \left(1 + \frac{\lambda_{1,i}}{\sin^2 \vartheta}\right)^{-1} \prod_{j=1}^{r_2} \left(1 + \frac{\lambda_{2,j}}{\sin^2 \vartheta}\right)^{-1} d\vartheta \quad (12)$$

$$\leq \frac{1}{2} \prod_{i=1}^{r_1} \frac{1}{1 + \lambda_{1,i}} \prod_{j=1}^{r_2} \frac{1}{1 + \lambda_{2,j}}, \quad (13)$$

upperbounded in (13) using $\sin^2 \vartheta \leq 1$.

We observe that each MS interleaves its own bits and the parity bits computed for the other MS before mapping them into symbols. It follows that the $d = d_1 + d_2$ non-zero bits of the error event \mathbf{c} can appear within the two time frames in several possible configurations, each corresponding to a different shift of \mathbf{c} at the input of the Viterbi decoder. To get an upperbound, we will select for each error event \mathbf{c} the most probable configuration among all these possible shifts by finding the one that maximizes (12).

B. Extension to imperfect inter-MS channel

In Sect. III-A, the average BER performance (for MS-1) has been analyzed only for the full cooperation case ($\Theta = 1$). The average BER over all the possible cooperation configurations $\Theta = \{1, 2, 3, 4\}$ can be evaluated as:

$$P_b \leq \frac{1}{k} \sum_{d \geq d_{\text{tr,ee}}} \sum_{\mathbf{c} \in \mathcal{E}(d)} \beta(\mathbf{c}) \left[\sum_{\Theta=1}^4 \Pr(\Theta) P(\mathbf{c} | \Theta) \right]. \quad (14)$$

The conditioned PEP $P(\mathbf{c} | \Theta = 1)$ for the full cooperation case is evaluated as in (12) - (13) based on the eigenvalue decomposition of the matrix (10). For the other cases $\Theta =$

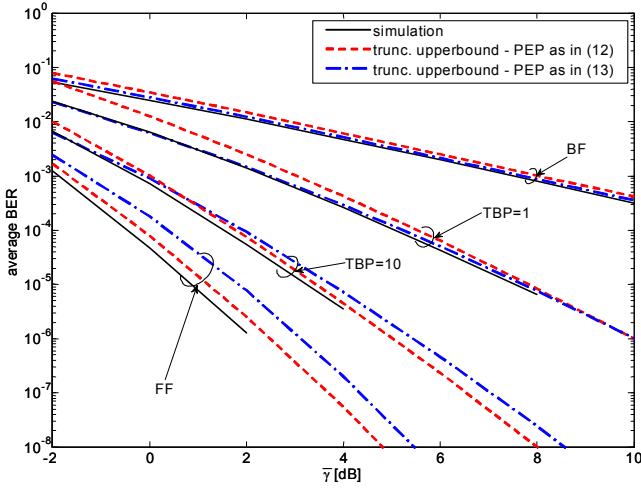


Fig. 5. Performance of full cooperation ($\Theta = 1$). Code-rate $R = 1/4$.

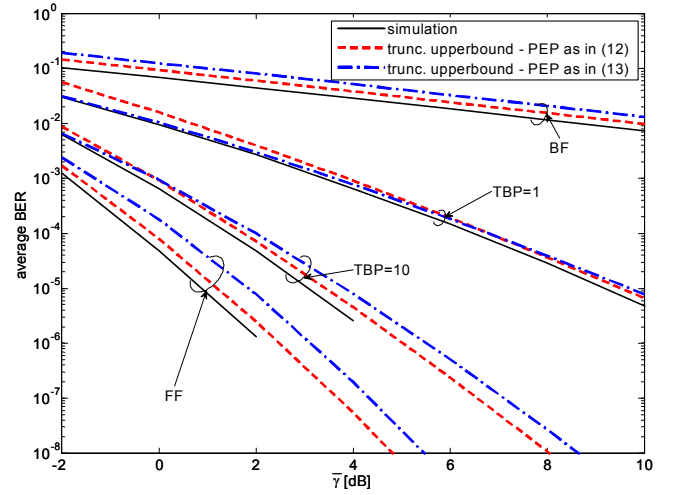


Fig. 6. Performance of no-cooperation ($\Theta = 2$). Code-rate $R = 1/4$.

$\{2, 3, 4\}$, the conditioned PEP can be obtained similarly using the eigenvalues of the following matrices:

$$\mathbf{R}_{\mathbf{c}}(\Theta = 2) = \begin{bmatrix} [\mathbf{R}_{\mathbf{c},1}]_{d_1 \times d_1} & [\mathbf{R}_{\mathbf{c},1}]_{d_1 \times d_2} \\ \left[[\mathbf{R}_{\mathbf{c},1}]_{d_1 \times d_2} \right]^H & [\mathbf{R}_{\mathbf{c},1}]_{d_2 \times d_2} \end{bmatrix}, \quad (15)$$

$$\mathbf{R}_{\mathbf{c}}(\Theta = 3) = \begin{bmatrix} \mathbf{R}_{\mathbf{c}}(\Theta = 2) & \mathbf{0} \\ \mathbf{0} & \mathbf{0} \end{bmatrix} + \begin{bmatrix} \mathbf{0} & \mathbf{0} \\ \mathbf{0} & [\mathbf{R}_{\mathbf{c},2}]_{d_2 \times d_2} \end{bmatrix}, \quad (16)$$

$$\mathbf{R}_{\mathbf{c}}(\Theta = 4) = [\mathbf{R}_{\mathbf{c},1}]_{d_1 \times d_1}, \quad (17)$$

where $[\mathbf{R}_{\mathbf{c},1}]_{d_2 \times d_2} = E[\tilde{\mathbf{h}}_{1,d_2} \tilde{\mathbf{h}}_{1,d_2}^H]$ is the auto-correlation of the MS-1 uplink channel gains associated to the d_2 second-frame error bits: $\tilde{\mathbf{h}}_{1,d_2} = \sqrt{E_s} [h_1(\tau_{\mathbf{c},d_1+1}) \cdots h_1(\tau_{\mathbf{c},d_1+d_2})]^T / \sigma_n$. The matrix $[\mathbf{R}_{\mathbf{c},1}]_{d_1 \times d_2} = E[\tilde{\mathbf{h}}_{1,d_1} \tilde{\mathbf{h}}_{1,d_2}^H]$ denotes the cross-correlation between $\tilde{\mathbf{h}}_{1,d_1}$ and $\tilde{\mathbf{h}}_{1,d_2}$. Notice that the sum in (16) is due to the assumption that the two sets of N_2 bits received from MS-1 and MS-2 during the second frame are optimally combined at the receiver using a maximum ratio combiner (MRC).

IV. SIMULATION RESULTS

In this Section we provide both numerical and analytical results on the performance of coded cooperation. The numerical results are obtained by Monte-Carlo simulations, BER results are obtained by averaging over a large number of frames. In Sect. IV-A, we validate the exact derivation (12) and the upperbound (13) on the average PEP by evaluating the average BER performance of coded cooperation for ideal inter-MS channel ($\Theta = 1$). Next, by removing the assumption of error-free inter-MS channel, more insight is given on the conditions for which coded cooperation can be regarded as competitive in terms of performance compared to non-cooperative (direct) transmission (Sect. IV-B): the cooperative regions for coded cooperation over time-varying channels are defined through examples.

A. Performance limits of coded cooperation

The results presented here refer to the case of ideal inter-MS channel, the best case for coded cooperation. The aim is to show the mobility conditions for which coded cooperation gains significantly. We employ a rate $R = 1/4$ RCPC mother-code [9], with octal generators (23, 35, 27, 33) and free distance $d_{\text{free}} = 15$. The mother-code is punctured, obtaining a rate $R_1 = 1/2$ sub-codeword for the first frame transmission ($\alpha = 50\%$). A soft-input hard-output Viterbi decoder is implemented at the receiver-side [11] and the error events \mathbf{c} are found via computer-enumeration. The coded-block length is $N = 512$ bits, resulting in $M = 256$ QPSK symbols. Before symbol mapping, the coded bits are interleaved by a block bit-interleaver, which writes the input codeword row by row in a (128×4) matrix, and then reads it column by column. The two MSs transmit on independent time-varying flat-fading channels with average SNR $\bar{\gamma}_i$ and time-bandwidth product TBP_i , with $i \in \{1, 2\}$. In Fig. 5, 6 and 7 the fading statistics are the same for both uplink channels, i.e. $\bar{\gamma} = \bar{\gamma}_i$ and $\text{TBP} = \text{TBP}_i$, which is almost true if the two MSs are moving at the same speed and are close to each other with respect to the location of the BS. The Clarke's model is implemented as in [14], [15, App. A].

In Fig. 5 and 6, the average BER performance of cooperative and non-cooperative systems is plotted versus the average SNR $\bar{\gamma}$ for different values of TBP. A vehicle-to-vehicle communication system is considered with carrier frequency $f_C = 5.2\text{GHz}$. The symbol duration is set to $T_S = 10\mu\text{s}$, this ensure that the channel's spectrum is flat². The time-bandwidth product TBP is chosen as performance metric to assess the degree of temporal variability of the channel (compared to the length of the codeword), as an example, when the MSs exhibit velocities up to $v = 160\text{km/h}$, the time-bandwidth product TBP goes proportionally up to 4. The analytical BER

²Recent channel measurements presented in [16] show that the delay spread at $f_C = 5.2\text{GHz}$ is around $1\mu\text{s}$.

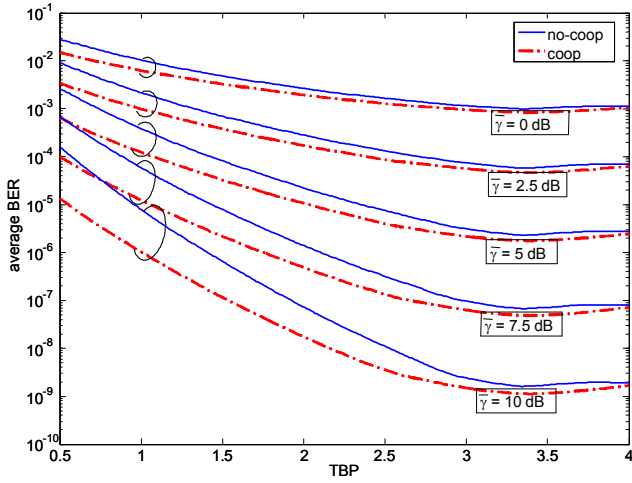


Fig. 7. Full cooperation ($\Theta = 1$) and no-cooperation ($\Theta = 2$) performance comparison. Code-rate $R = 1/4$.

bounds are computed by truncating the first summation in (5) at $d = 23$, or at values that are smaller but sufficient to upper bound the simulation results. The average PEP is computed both according to (12) and (13), (for the latter we truncate (5) at $d_{\text{free}} = 15$). We observe that the performance for increasing TBP moves to the one obtained for FF.

In Fig. 7 the bounds on the average BER are plotted versus the TBP. Coded cooperation and no-cooperation are compared at different average SNR values $\bar{\gamma}$. Up to $\text{TBP} \approx 3$ ($v = 120\text{km/h}$), the performance gain of coded cooperation increases with increasing average SNR. At higher velocities the gain is almost negligible, which means that benefits of coded cooperation vanish for $\text{TBP} \gtrsim 3$.

We analyze now the case where the uplink channels are unbalanced (thus showing different values of average SNR and/or velocity). In Fig. 8 MS-1 moves at $\text{TBP}_1 = 1$ and transmits on a channel with average SNR $\bar{\gamma}_1 = 10\text{dB}$. On the other hand, average SNR for MS-2 varies from 5dB to 10dB, and time-bandwidth product $\text{TBP}_2 = \{0, 0.5, 1\}$. The performance results suggest that coded cooperation outperforms remarkably no-cooperation only if the MSs are moving approximately at the same speed. The larger is the difference between MSs' velocities, the less advantageous it is for the fastest MS to cooperate. This result can be useful in case partner selection can be allowed [4].

We argue that the conclusions drawn in this Section are valid for every good RCPC code, because the diversity gain is carried by the cooperation scheme (space-diversity) and the bit-interleaving (time-diversity), independently from the specific code.

B. Cooperative regions

We now consider the more realistic case of imperfect inter-MS channel. We also adopt a RCPC code with higher rate than the one in Sect. IV-A to allow for a reasonable simulation complexity. The adopted RCPC mother-code, with octal

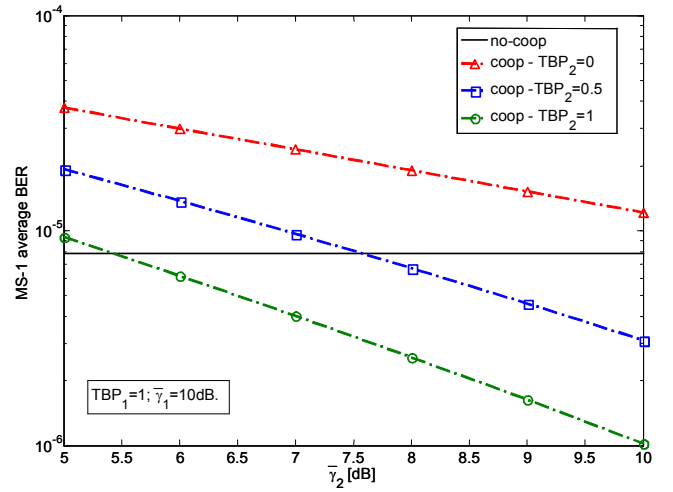


Fig. 8. Performance of MS-1 for asymmetric uplink channel conditions: MS-1 moves with $\text{TBP}_1 = 1$ and $\bar{\gamma}_1 = 10\text{dB}$; MS-2 moves at different velocities with varying $\bar{\gamma}_2$. Full coded cooperation and no-cooperation are compared. Code-rate $R = 1/4$.

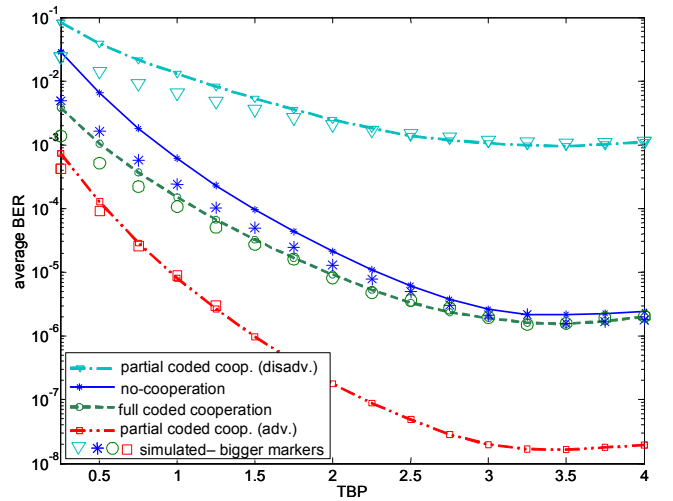


Fig. 9. Performance of the four cases of coded cooperation at $\bar{\gamma} = 7.5\text{dB}$: truncated bounds and simulation results. Partial cooperation is advantageous or disadvantageous from the point of view of one MS. Code-rate $R = 1/3$.

generators (15, 17, 13), has rate $R = 1/3$ and free distance $d_{\text{free}} = 10$. The coded-block length is $N = 384$ bits, resulting in $M = 192$ QPSK symbols. The punctured code has rate $R_1 = 1/2$, with code-length $N_1 = \frac{2N}{3}$ ($\alpha \simeq 33\%$). The coded bits are interleaved by a block bit-interleaver (96×4). Average BER performance for the four cases of coded cooperation (see Sect. II) are depicted in Fig. 9 for an average SNR of both uplink channels $\bar{\gamma} = 7.5\text{dB}$ and varying degree of temporal variability TBP. In accordance with the results in Sect. IV-A, the coded cooperation (for the case $\Theta = 1$) does not provide any significant gain with respect to non-cooperative case for $\text{TBP} \geq 3$. The upperbound (5), with PEP computed as in (12) and error event autocorrelation matrices according to (10) and (15) - (17), are truncated at $d = 14$,

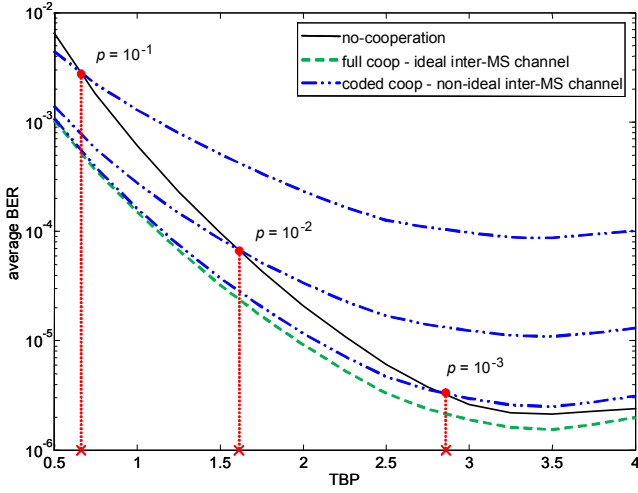


Fig. 10. Performance of coded cooperation at different inter-MS block error probability p compared to no-cooperation at $\bar{\gamma} = 7.5\text{dB}$. Code-rate $R = 1/3$.

or at smaller values, in order to get tighter bounds for the subsequent analysis. These bounds are weighted as in (14) for different values of the inter-MS block error probability p and compared to no-cooperation in Fig. 10. As far as the mobility degree becomes large enough, the average BER performance of coded cooperation with non-ideal inter-MS channel is increasingly dominated by the worst case partial cooperation ($\Theta = 4$), as expected. The comparison between cooperative and non-cooperative transmission in terms of BER performances shows that the mobility degree threshold (cross markers in Fig. 10), beyond which coded cooperation is no more advantageous, decreases with decreasing quality of the inter-MS channel. For instance, coded cooperation with inter-MS block error probability $p = 10^{-3}$ is advantageous only up to $\text{TBP} \approx 2.5$ for the considered code and channel settings. Furthermore, analytical and numerical results reveal that this threshold strongly depends on the quality of the relayed links ($\bar{\gamma}$).

The *cooperative region* is the collection of mobility (TBPs) and channel ($\bar{\gamma}$, p) settings for which coded cooperation is beneficial in providing enhanced average BER performance with respect to the non-cooperative case. The cooperative regions are illustrated as shaded areas delimited by solid lines in Fig. 11. For different values of the average SNR $\bar{\gamma}$, shaded areas contain the collection of values (TBP, p) for which coded cooperation provides superior performances compared to non-cooperative transmission. Interestingly, we observe that, for $\bar{\gamma} < 10\text{dB}$, the cooperative region spans the entire TBP range considered: the most promising opportunities to exploit the benefits of coded cooperation (in time-varying fading) arise for those applications where energy efficiency (for low SNR) is a key issue. Reasonably, the cooperative region size increases (decreases) with decreasing (increasing) average SNR $\bar{\gamma}$. In Fig. 12, the cooperative region for MS-1 is depicted by assuming the uplink channels with average SNR $\bar{\gamma} = 10\text{dB}$,

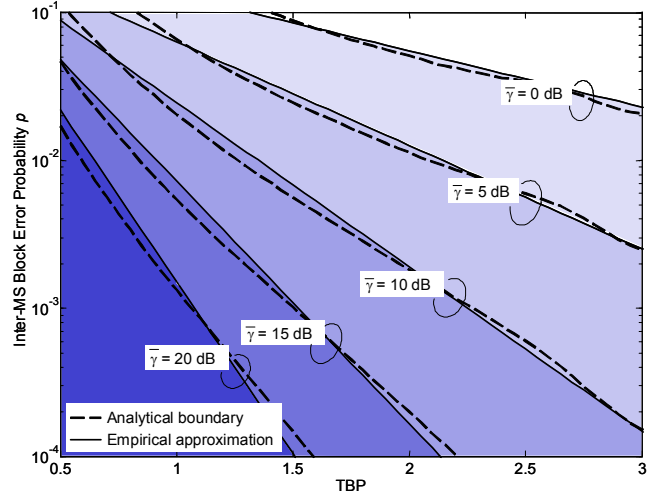


Fig. 11. *Cooperative regions* for coded cooperation at different $\bar{\gamma}$. Coded cooperation outperforms no-cooperation in the region below the analytical boundary. Code-rate $R = 1/3$.

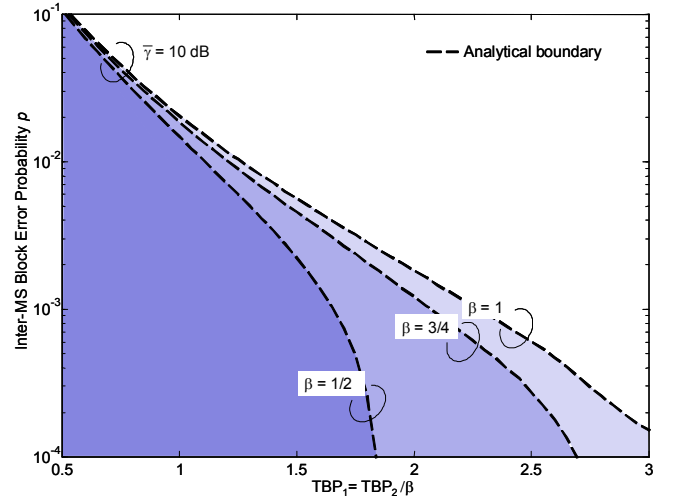


Fig. 12. *Cooperative regions* for MS-1. Uplink channels are both at $\bar{\gamma} = 10\text{dB}$, but MS-2 velocity is β times smaller than MS-1 velocity. Code-rate $R = 1/3$.

while the degree of mobility of MS-2 is lower compared to MS-1 as $\text{TBP}_2 = \beta \times \text{TBP}_1$ with $\beta < 1$. As expected from the analysis in Sect. IV-A, the cooperative region for MS-1 becomes smaller if the partner moves at lower velocities ($\text{TBP}_2 < \text{TBP}_1$).

V. CONCLUSIONS

We have provided an analytical method to evaluate the average BER performance of coded cooperation over time-varying flat fading channels. The key idea lies in recognizing the algebraic structure of the fading channel autocorrelation matrix associated to the decision variable. The theoretical results have been corroborated and validated by simulation results. The present work has focused on a generic single-carrier transmission system with narrowband channels, but

the methodology can be transposed to broadband frequency-selective OFDM systems taking into account the correlation of the fading channel over the subcarriers. The analysis has at first encompassed the widest range of temporal variability of the fading process, from the BF to the FF model. However, the temporal variability strictly depends on the velocity of the mobile stations, which is necessarily limited. This physical limitation has been taken into account by circumscribing the performance evaluations to a more realistic range of temporal variability of the channel.

Analytical results, validated by simulations, have shown that coded cooperation, in the best case of error-free inter-MS channel, outperforms significantly a comparable non-cooperative transmission only up to a certain degree of mobility, approximately when the time-bandwidth product $TBP \lesssim 3$ (corresponding to the speed $v = 120\text{km/h}$ in a system with carrier frequency $f_C = 5.2\text{GHz}$, symbol duration $T_S = 10\mu\text{s}$ and code block length $M = 256$ symbols). Beyond this limit, coded cooperation and non-cooperative transmissions perform similarly, since the gain offered by the time diversity is now dominant.

We have also investigated how the MSs' speed difference and the degradation of the inter-MS channel quality affect the BER performance. As expected, the larger is the speed difference the less advantageous it is to cooperate for the fastest MS. However, it has been shown that, for the MS moving at twice the velocity of the partner, coded cooperation improves significantly the performance with respect to no-cooperation up to $TBP \simeq 1.5$ ($v = 60\text{km/h}$). Furthermore, the increase of the inter-MS block error probability has been proven to be a penalty factor for coded cooperation performance. For instance, coded cooperation in symmetric uplink channels' conditions performs better than no-cooperation at $TBP = 2.5$, average SNR $\bar{\gamma} = 10\text{dB}$ and inter-MS block error probability $p = 10^{-4}$, while performing worse as the inter-MS block error probability raises to $p = 10^{-3}$. The *cooperative region* have been derived in order to provide more insight to the analysis by defining the mobility and channel settings for which coded cooperation provides better performance than no-cooperation. The proposed approach can be used in network design in order to define algorithms for the selection of the cooperating MSs and the optimization of the cooperation level [4].

We believe that the present work contributes to build the base for future evaluations of coded cooperation in real mobile communication systems, with the support of detailed channel and mobility models.

ACKNOWLEDGEMENTS

This work was supported by the European Project #IST-216715 Network of Excellence in Wireless Communications (NEWCOM++), the Vienna Science and Technology Fund in the ftw. project COCOMINT, and the Austria Science Fund (FWF) through grant NFN SISE (S106). The Telecommunications Research Center Vienna (ftw.) is supported by the Austrian Government and the City of Vienna within the competence center program COMET.

REFERENCES

- [1] J. N. Laneman, D. N. C. Tse and G. W. Wornell, "Cooperative diversity in wireless networks: efficient protocols and outage behavior," *IEEE Trans. Inform. Theory*, vol.50, pp.3062-3080, Dec. 2004.
- [2] T. E. Hunter and A. Nosratinia, "Cooperation diversity through coding," in *Proc. IEEE ISIT*, July 2002, p. 220.
- [3] D. Tse and P. Viswanath, *Fundamentals of Wireless Communication*, Cambridge University Press, 2005.
- [4] S. Valentin and H. Karl, "Effect of user mobility in coded cooperative systems with joint partner and cooperation level selection," in *Proc. IEEE WCNC*, March 2007, pp. 896-901.
- [5] Z. Lin, E. Erkip, A. Stefanov, "Cooperative regions and partner choice in coded cooperative systems," *IEEE Trans. Commun.*, vol. 54, pp. 1323-1334, Jul. 2006.
- [6] J. Proakis, *Digital Communications*, 4th Ed., McGraw Hill, 2001.
- [7] K. Witralsal, Y. Kim, R. Prasad, "A novel approach for performance evaluation of OFDM with error correction coding and interleaving," in *Proc. IEEE VTC Fall*, Sep. 1999, Vol. 1, pp. 294-299.
- [8] D. Molteni, M. Nicoli, R. Bosisio, L. Sampietro, "Performance analysis of multiantenna WiMax systems over frequency-selective fading channels," in *Proc. IEEE PIMRC*, Athens, Sep. 2007.
- [9] J. Hagenauer, "Rate-compatible punctured convolutional codes (RCPC codes) and their applications," *IEEE Trans. Commun.*, vol. 38, pp. 389-400, Nov. 1988.
- [10] R. H. Clarke, "A statistical theory of mobile-radio reception," *Bell Syst. Tech. J.*, p. 957, Jul.-Aug. 1968.
- [11] S. Lin and J. D. Costello, *Error Control Coding - Fundamentals and Application*, Prentice-Hall, 2003.
- [12] M.K. Simon, M.S. Alouini, *Digital communications over fading channels: a unified approach to performance analysis*, Wiley, 2000.
- [13] J. W. Craig, "A new, simple, and exact result for calculating the probability of error for two-dimensional signal constellations," in *Proc. IEEE MILCOM*, Nov. 1991, vol. 2, pp. 571-575.
- [14] Y. R. Zheng and C. Xiao, "Simulation models with correct statistical properties for Rayleigh fading channels," *IEEE Trans. Commun.*, vol. 51, no. 6, pp. 920-928, June 2003.
- [15] T. Zemen and C. F. Mecklenbräuker, "Time-variant channel estimation using discrete prolate spheroidal sequences," *IEEE Trans. Signal Processing*, vol. 53, no. 9, pp. 3597-3607, Sep. 2005.
- [16] A. Paier et al, "Non-WSSUS vehicular channel characterization in highway and urban scenarios at 5.2 GHz using the local scattering function," in *Proc. IEEE WSA*, Darmstadt, Germany, Feb. 2008.